

1    **Development of a World-Wide Database of Atoll Morphometrics**

2    **Enter authors here: Faith M. Johnson<sup>1</sup> and Alejandra C. Ortiz<sup>2,1</sup>**

3    <sup>1</sup>Department of Civil, Construction, and Environmental Engineering, North Carolina State  
4    University, Raleigh, NC 27695

5    <sup>2</sup>Department of Geology, Colby College, Waterville, ME 04901

6    Corresponding author: Alejandra C. Ortiz ([acortiz@colby.edu](mailto:acortiz@colby.edu))

7    **Key Points:**

- 8       • Global Atoll Morphometric Database created for 154 Atolls, 3,795 motu, and 596 reef  
9       flats
- 10      • Development python code for automated morphometric analysis of satellite imagery of  
11      atolls
- 12      • For all motu larger than 1 km (n = 725), consistent reef-flat width in front of motu of 188  
13      ± 156 m

14    **Abstract**

15    Small Island Nations are at considerable risk of climate change impacts from sea-level rise to  
 16    coral acidification to increasing cyclone intensity; understanding how they will change in the  
 17    coming century is vital for climate mitigation and resiliency. Atoll morphometrics are calculated  
 18    for 3,795 motu and 593 reef flats on 154 atolls. The total land (motu) area is 1,836.55 km<sup>2</sup> with a  
 19    total reef flat area of 7,387.43 km<sup>2</sup>. A consistent methodology to classify, segment, and calculate  
 20    morphometrics is used. Composites are created for 4 years (2015- 2018), and are classified into  
 21    motu, reef flat, open water/lagoon via unsupervised classification. Morphometrics are computed  
 22    for each motu and reef flat of the atoll in python, creating a database of atolls and their  
 23    associated morphometrics. Consistency in processing removes spatial and user bias, enabling a  
 24    better understanding of geographic patterns of atolls. We identify trends in atoll, motu, and reef  
 25    flat formations. The average atoll reef flat width is  $850 \pm 817$  m and the average motu width is  
 26     $263 \pm 210$  m. Distinct differences in the distribution of motu can be seen on a regional scale in  
 27    French Polynesia, while globally, wider reef flats with larger motu are found closest to the  
 28    equator. Globally there is a consistent reef flat width in front of large motu (> 10 km length) of  
 29     $188 \pm 156$  m. Our atoll morphometric database creates a baseline of current atoll characteristics  
 30    that can be expanded upon in the future and used for evaluating temporal changes to atoll  
 31    islands.

32    **Plain Language Summary**

33    To understand what will happen to small island nations under climate change, we must  
 34    understand the current state of these islands. We have created a method in python code to  
 35    automatically take a satellite image of an atoll, a tropical island where an old reef surrounds an  
 36    inner lagoon with small islets (motu) on top, and classify into land, water, and reef. Our code  
 37    then automatically measures characteristics of these landscapes like the area of each motu (islet)  
 38    or the width of each reef-flat for 3,791 motu and 593 reef flats on 154 atolls. In French  
 39    Polynesia, there is a consistent pattern of large motu appearing on the north and eastern side of  
 40    the atoll with a narrower total reef-flat width found on these sides. Globally, a consistent reef-flat  
 41    width in front of the motu is found to be  $188 \pm 156$  m. These measurements allow a current  
 42    snapshot atoll measurements, which can be used as a baseline to track potential impacts of  
 43    climate change by measuring changes to these landscapes over time.

44    **1 Introduction**

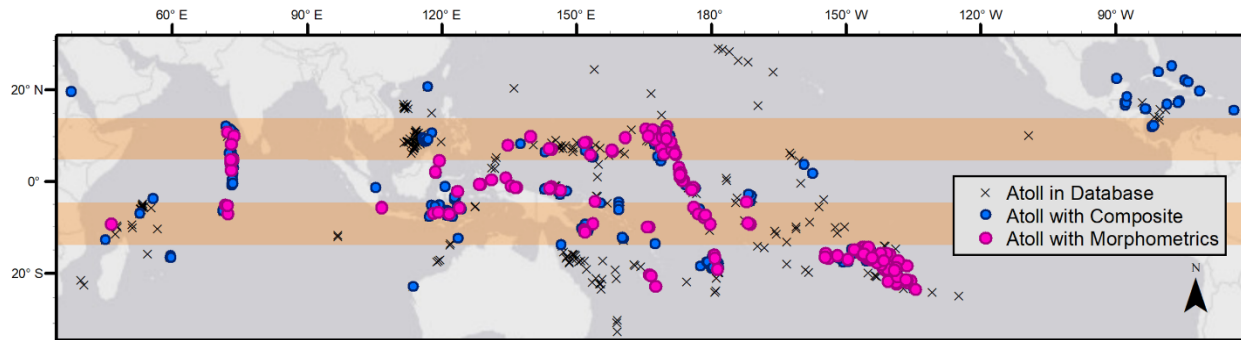
45    The sub-aerial land found atop atoll carbonate reef platforms, known as reef islands,  
 46    islets, motu, and cays, often serve as the only home to terrestrial ecosystems and human  
 47    infrastructure on remote island nations. Despite their essential role, the morphologic processes  
 48    shaping and forming these islets remain poorly understood. Moreover, a consistent method for  
 49    measuring their current morphometrics is lacking (Duvat, 2019). To predict the response of these  
 50    island nations to rising sea levels and other climate change impacts (Barnett & Adger, 2003;  
 51    Fletcher & Richmond, 2010; Kumar, 2020), we must first create a baseline of planform land area  
 52    and a reproducible method for measuring change.

53    We create a series of python scripts utilizing Google Earth Engine and Landsat imagery  
 54    to measure atoll morphometrics such as motu area or reef-flat width. Our robust methodology  
 55    employs open-source software and allows for a consistent approach to calculating planform  
 56    terrestrial area of these island nations and a path for measuring and tracking changes to these  
 57    landscapes over time. By investigating the regional and global patterns of atoll morphometrics

58 along with previous hydrodynamic modeling (Ortiz & Ashton, 2019), we develop a conceptual  
 59 model to explain differing pathways of motu and reef flat evolution.

60 **1.1 Background**

61 Atolls are found in tropical oceans, consisting of a carbonate reef platform (hereafter  
 62 called reef flat) surrounding a central lagoon with subaerial islands on top of the reef (hereafter  
 63 called motu) (Schlager & Purkis, 2013). We use a broad and inclusive definition of an atoll: a  
 64 carbonate reef-platform encircling or partially surrounding a central lagoon (which may or may  
 65 not be filled in), emplaced upon may be subaerial landforms. With this broad definition, our atoll  
 66 database includes 623 atolls, easily subsetted down based on a range of factors (e.g. only atolls  
 67 containing motu); this broad definition was done to ensure that all possible island forms are  
 68 captured in our analysis (Figure 1).



69  
 70 Figure 1. Map of atolls worldwide showing locations of atolls in database (black x), atolls with composite imagery  
 71 created from Landsat (blue dots), and atolls with both composite imagery and morphometrics calculated (pink dots),  
 72 separated into equatorial ( $0^{\circ}$ - $4.7^{\circ}$  latitude), mid tropical ( $4.7^{\circ}$  -  $14^{\circ}$  latitude) highlighted in beige strips, and high  
 73 tropical ( $14^{\circ}$  -  $27^{\circ}$  latitude).

74 Atolls are formed from coral reefs growing on subsiding dormant volcanic islands  
 75 (Darwin, 1842) and are shaped through global changes in sea levels (Daly, 1925; M. R. Toomey  
 76 et al., 2016). Motu (aka cays or islets) are composed of carbonate sand, coral shingle, and rubble  
 77 perched on top of the conglomerate reef flat encircling the inner lagoon (Woodroffe et al., 1999).  
 78 Similar to Ortiz and Ashton (2019), we do not limit the term motu to only islets comprised of  
 79 particular sediment sizes as suggested by some authors (Brander et al., 2004; Paul Simon Kench  
 80 et al., 2017; Richmond, 1992) as the distinction varies across papers. Motu form and evolve on a  
 81 shorter time scale, decades to centuries (Paul Simon Kench, Owen, et al., 2014; Perry et al.,  
 82 2013; C D Woodroffe et al., 1999), than the atoll itself, millennia to hundreds of thousands of  
 83 years (M. Toomey et al., 2013; M. R. Toomey et al., 2016). Motu initiation, formation, and  
 84 evolution has occurred under current (Paul Simon Kench, Chan, et al., 2014; Sengupta et al.,  
 85 2021), rising (Paul S Kench et al., 2005; McLean & Kench, 2015a; Webb & Kench, 2010), and  
 86 falling sea level conditions (Colin D. Woodroffe et al., 2007). Evolution of motu can be episodic,  
 87 with island change tied to specific events such as a tropical cyclone that added sediment to the  
 88 system (Duvat & Pillet, 2017) or land reclamation from human activities (Aslam & Kench,  
 89 2017a; Duvat & Magnan, 2019; Duvat & Pillet, 2017; M. Ford, 2011).

90 Atolls are at risk from climate change due to their low-lying nature; many atolls have a  
 91 maximum elevation of less than 5 m. Accelerated rates of sea-level rise (SLR) may outpace  
 92 vertical reef flat accretion from the coral reefs. In addition, storm driven flooding will be  
 93 increased by climate change (Storlazzi et al., 2015) driving increased flooding and inundation

94 from swell waves generated by distant storms (Hoeke et al., 2013; Shope et al., 2017). Ocean  
 95 acidification and other oceanographic stressors such as changing ocean temperature can reduce  
 96 sediment production from the coral reefs putting the ability of motu and reef platforms to keep  
 97 pace with SLR further at risk (Eyre et al., 2018). To understand the potential response of these  
 98 landforms to changing climate risks, we must first understand the processes driving their  
 99 evolution and their current state.

100 Although atolls are often described as circular or annular structures, their morphology  
 101 varies widely. The controls on atoll shape are poorly understood and inconsistently quantified.  
 102 Previous work by Stoddart (1965) used hand tracing of 99 atolls to measure their shape,  
 103 demonstrating a “fundamental homogeneity of atoll shapes” including a tendency for elongated  
 104 and more elliptical atolls rather than the often described ring-shape. Our methods recreate these  
 105 measurements both at the atoll scale and at the individual motu or reef-flat scale, enabling further  
 106 study of atoll island change and comparison between current and previous measurements.

107 Many studies of atoll geomorphology use a combination of field and remote sensing  
 108 technologies, including historic aerial photography and modern satellite imagery, ranging from a  
 109 focus on one motu to a regional group of atolls. Frequently studies have relied on hand digitation  
 110 of shorelines and atoll morphology (Duvat & Pillet, 2017; M. R. Ford & Kench, 2014, 2015;  
 111 Paul Simon Kench, Chan, et al., 2014; Sengupta et al., 2021; Webb & Kench, 2010). Different  
 112 features are used as a proxy for the shoreline location including edge of vegetation (Albert et al.,  
 113 2016a; M. R. Ford & Kench, 2015; Garcin et al., 2016)), defining a stability line (Duvat & Pillet,  
 114 2017), using a GPS track at the time of the field work (Paul Simon Kench, Chan, et al., 2014),  
 115 using supervised classification (Holdaway et al., 2021), and using an image analysis software  
 116 with hand digitation to fix any errors (Schlager & Purkis, 2013). Studies looking at changes in  
 117 land area or shoreline position on atolls include (Albert et al., 2016b; Aslam & Kench, 2017b;  
 118 Duvat & Magnan, 2019; Duvat & Pillet, 2017; Paul S Kench et al., 2018; McLean & Kench,  
 119 2015b; Nunn et al., 2020). Ford and Kench (2014) examined changes on Nadikdik Atoll in the  
 120 Marshall Islands using remote sensing data from 1945–2010. Using the edge of vegetation, as  
 121 proxy for shoreline, they found a net increase of island area including the formation of a new  
 122 island from an initial deposit of sediment to a stable island with vegetation.

123 Duvat (2019) re-analyzed 20 different papers studying atoll land area change for 30 atolls  
 124 (709 islands). They found that 88.6% of the islands were stable (within +/- 3% area change) or  
 125 increased in area over the time period of analysis. All the larger islands (> 0.1 km<sup>2</sup>) were either  
 126 stable or increased in area. A key aspect of this paper is the collation of other studies and  
 127 comparison atoll island changes across decadal changes. One of their stated future research  
 128 priorities is to create a common assessment protocol to strengthen data comparability, which our  
 129 research directly addresses. Holdaway et al. (2021) leveraged large amounts of available satellite  
 130 imagery to quantify atoll land area change for 221 atolls. Similar to our procedure, they created  
 131 temporal composites of atolls from Landsat imagery with a mix of multiyear and annual  
 132 composites. Supervised classification, with a fluctuating number of landcover classes, was used  
 133 to segment the images. For comparison between all the sites, a binary land/water class was  
 134 created and total land area change was calculated on an atoll level. From 2000 – 2017, land area  
 135 increased 6.1% for the 221 atolls, primarily in the Maldives and South China Sea mainly due to  
 136 land reclamation (Holdaway et al., 2021).

137 Numerical modeling work by Ortiz and Ashton (2019) found that the width of the reef-  
 138 flat in front of motu (the distance from the oceanside of the motu to the edge of the oceanside of  
 139 the reef-flat) should reach an equilibrium distance dependent on the offshore wave climate.

140 Using the open-source model XBeach in hydrodynamic mode, they investigated the potential  
 141 response of sediment transport with the presence of a 1D motu to changing offshore wave  
 142 climate and changing reef-flat widths in front of the motu. They found that once motu are present  
 143 on the reef flat (i.e. once there sub-aerial land blocking the reef-flat from the lagoon), the motu  
 144 would grow and accrete oceanward (thus narrowing the oceanside motu to reef-flat width) up to  
 145 a certain point where the direction of sediment transport would reverse and direct sediment  
 146 offshore. Their conceptual model predicts self-organization of motu prograding oceanwards to a  
 147 critical reef-flat width dependent on the offshore wave height. 2D modeling by Shope and  
 148 Storlazzi (2019) found that that atoll islands orientated parallel to the deep-water wave direction  
 149 would accrete towards the lagoon while eroding along shorelines exposed to direct wave action.

150 While there are many studies of atolls island evolution, there is a critical need to establish  
 151 a baseline of atoll morphometrics using a consistent methodology. The aim of this research is to  
 152 create a reproducible approach to evaluate atoll morphology on a broad spatial scale using  
 153 satellite imagery and innovative data processing techniques. We use a constant time frame for  
 154 the temporal composites, an automated classification technique to separate the atoll into parts  
 155 (motu, reef flat, open water/lagoon), automatically segmenting the classified imagery, and  
 156 calculating morphometrics on each object. We create a worldwide database of atolls and their  
 157 morphometrics. This methodology removes spatial bias and enables a better understanding of  
 158 current geographic patterns in atoll morphometrics and potentially identify first order patterns  
 159 between atolls.

## 160 2 Materials and Methods

161 Our code is built on open-source software within python using common libraries in  
 162 image analysis (i.e. Google Earth Engine, skimage, and pandas) to create temporal composites,  
 163 classify into three landcover classes, and segment into objects for morphometric analyses. We  
 164 have created a suite of python scripts with discrete morphometric calculating functions, available  
 165 on GitHub ([AtollGeoMorph](#)), that other users can adapt for their own morphometric analysis.  
 166 For each atoll, a temporal composite is created then classified into land, water, or reef-flat using  
 167 k-means unsupervised classification. These landcover classes are then segmented and analyzed  
 168 for a variety of morphometrics including area, width, centroid, and length (Figure 2). From these  
 169 morphometrics, we calculate atoll-scale averages as well as bin by cardinal position on the atoll.  
 170 Our database allows easy comparison at the individual atoll-scale, object-scale (i.e. comparing  
 171 all the motu widths measured), the regional scale (patterns of motu widths in French Polynesia),  
 172 or globally.

### 173 2.1 Composites and Classification

174 Four-year temporal composites (2015 - 2018) are created from Tier 1 Landsat Images  
 175 using the Google Earth Engine library (GEE) in python similar to the methodology used by Ortiz  
 176 et al. (2017). For a given atoll, all Tier 1 Landsat images available from 2015-2018 are  
 177 collected, cloudy pixels are removed using in-built GEE cloud removal functions, and the  
 178 remaining pixels from each image are composited using the 50<sup>th</sup> percentile on a per-pixel per-  
 179 band basis. Tier 1 Landsat images are georectified, have atmospherically corrected surface  
 180 reflection, and have a 30 meter resolution (Google Earth Engine Team, 2015). Six bands (blue,  
 181 green, red, NIR, SWIR1, and SWIR2) are retained in our final temporal composite. A count band  
 182 indicating the number of images used for the composite in each pixel and a mask band to show

183 the geometry given to GEE are also included. This composite is saved as a geotiff for easy access  
 184 by other scripts. The temporal composite method has been used by other researchers as it can  
 185 remove issues of cloudiness in a given Landsat image, a very common issue for Atolls (Mateo-  
 186 García et al., 2018; Ortiz et al., 2016).

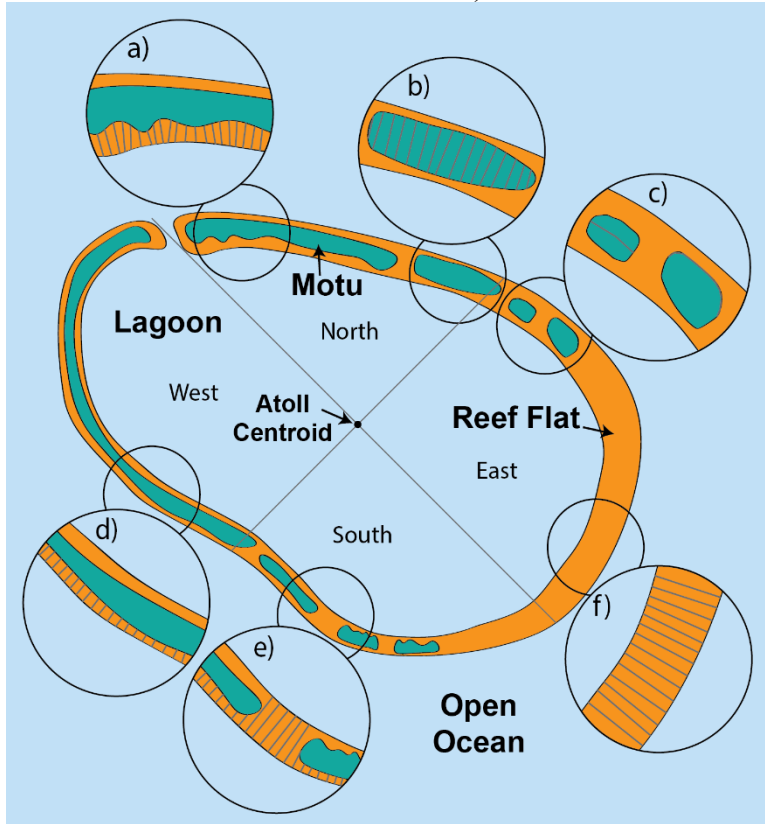


Figure 2. Conceptual diagram of morphometrics calculated for idealized atoll classified into three landcovers: green (subaerial land, motu), orange (reef flat), and blue (water). A) Motu to lagoon-side reef-flat width (herein called lagoon reef width), b) motu width, c) motu length, d) motu to ocean-side reef-flat width (herein called ocean reef width), e) effective reef-flat width, and f) total reef-flat width (assuming no land on top, herein called reef-flat width).

Approximate location of center of mass of entire atoll object denoted by atoll centroid with resultant segregation of atoll objects by cardinal directions North, East, South, and West shown.

208

We assume that the primary

209 landcover classes on an atoll are reef flat, motu (land), and water and use k-means clustering for  
 210 automated classification. The mask from the composite is used to remove any edge issues or  
 211 other nearby atolls. Given Landsat's medium resolution (30 m), the classified image is cleaned  
 212 by removing small groups with less than 8 isolated pixels (objects < 7,200 m<sup>2</sup> are not analyzed).  
 213 All motu smaller than 7,200 m<sup>2</sup> but smaller than 57,600 m<sup>2</sup> (64 isolated pixels), only have  
 214 basic morphometrics calculated (area, perimeter, and location), while motu larger than 64 pixels  
 215 have complex morphometrics calculated (such as width and length). The total area across our  
 216 entire database accounted for by motu between .72 and 5.7 hectares, 8-64 connected pixels (n =  
 217 2,036), is less than 3% of the total area (47 km<sup>2</sup>) measured by the remaining large motu (n =  
 218 1,753, 1,789 km<sup>2</sup>). The morphometric analysis is run on the cleaned classified temporal  
 219 composite with all the resultant data saved in pandas dataframes and as CSV files.

## 220 2.2 Morphometrics

221 A methodology for determining atoll morphometrics is created and implemented in python  
 222 scripts, publicly available on GitHub (<https://github.com/ale37911/AtollGeoMorph>). Our python  
 223 scripts are split into three distinct pieces: 1) create temporal composites (Section 2.1), 2) classify,  
 224 clean, and segment the image then calculate morphometrics (Section 2.2), and 3) collate saved  
 225 outputs from each atoll into larger dataframes for analysis and visualization (Section 3.3). For

226 detailed description of the methods used in the morphometric analysis see Supporting  
 227 Information Text S1.

228 Once classified, the number and approximate location of lagoons is input by the user.  
 229 Users manually close the lagoon for cases where automated lagoon finder is unable to match the  
 230 lagoon number. Morphometrics of the lagoons are calculated: area, perimeter, all the perimeter  
 231 points (on a per-pixel basis), and the centroid. Atoll level morphometrics are also calculated:  
 232 outside atoll perimeter (ocean perimeter), the atoll centroid, and shape factors used by Stoddart  
 233 (1965). Area, perimeter, and centroid of each object (i.e. reef flat or motu) are calculated and  
 234 stored in pandas dataframe where each row is the perimeter point per object (motu or reef flat)  
 235 basis. All points are classified as an ocean-side or lagoon-side point based on relative distances  
 236 to the lagoon or ocean.

237 For each point, several morphometrics are calculated from an exposure angle to a cardinal  
 238 position angle along with multiple widths within each object, i.e. width of a motu or total width  
 239 of a reef-flat per point from ocean-side to lagoon-side, or between objects, i.e. width from motu  
 240 ocean-side point to reef-flat ocean side points called ocean reef width (Figure 2, Figure S1). The  
 241 width code utilizes a list of points for calculating the width (i.e. ocean-side perimeter points of a  
 242 motu), the associated shoreline exposure angles for those points, and a list of points the width  
 243 will be calculated to (i.e. lagoon-side perimeter points for the same motu). It finds the nearest  
 244 perpendicular point (i.e. on the lagoon side) within a range of degrees, assuming a default 15°.

245 The length of each motu is calculated using the center points of motu width measurements  
 246 (Figure 2). The motu length is calculated as the cumulative distance along that line. The ocean-  
 247 side and lagoon-side lengths are also. For the reef length, the ocean side length is used as proxy  
 248 for the length. Since the reef flat ocean side points may not be in order, any points that are more  
 249 than 3 pixels apart are skipped in the length sum. After processing the motu, reef flat, and lagoon  
 250 data frames are saved to CSV and excel spreadsheets.

### 251 2.3 Analysis at range of Scales

252 Atolls are analyzed individually, regionally, and globally with morphometrics summarized  
 253 at a per-point, per-object, and per-atoll level. At the region level, morphometrics are also binned  
 254 by cardinal direction relative to the atoll centroid (positioning angle), while at the global scale  
 255 morphometrics are binned by absolute latitude. Summary tables are created for each atoll that  
 256 include at least the area, mean widths, length, centroid location, cardinal directional bin  
 257 (positioning angle bin) most of the object is in for each of motu, reef flat, and lagoon object. By  
 258 using pandas dataframes, it is relatively easy to summarize the data based on different grouping  
 259 criteria such as latitude or country or even selected atoll names. We have selected several  
 260 methods for analyzing our dataset but expect that other groupings could be used to identify  
 261 patterns in the database. Primary morphometrics for all 154 atolls analyzed are available as a  
 262 table (Table S1). In addition, the code to create all morphometrics are available  
 263 (AtollGeoMorph).

## 264 3 Results

265 There are 623 atolls in our inclusive atoll database. There is adequate Landsat coverage to  
 266 create a composite for 385 of those atolls, of which we calculate morphometrics for 154 (Figure  
 267 1). We started with an inclusive list of atolls including some with no motu (fully submerged  
 268 reefs), interior islands in the lagoon (i.e. Bora Bora, French Polynesia), or that had very small or  
 269 completely filled in lagoons (i.e. Nikunau, Kiribati). While we were able to create a composite

270 for some of these atolls, they were not included in the morphometrics calculations. Results are  
 271 presented for Faaite Atoll in French Polynesia, regionally for French Polynesia, and globally for  
 272 all atolls analyzed.

273 3.1 Atoll Scale Results: Faaite Atoll, French Polynesia



274  
 275 Figure 3. Faaite atoll, French Polynesia object level data. Background image is K-means classified with individual  
 276 objects labeled: motu are green (all morphometrics calculated) and yellow (small motu, only basic morphometrics  
 277 calculated), reef flat are blue, and water is purple. Motu are labeled starting with M, reef flats with R, and the lagoon  
 278 with L. This letter is followed by the index number assigned north to south for each class of object based on the  
 279 northern most point of that object. Morphometric summary tables are included for a) reef flats, b) lagoons, and c)  
 280 motu. Error in the mean widths is one standard deviation.  
 281

282 Faaite Atoll, French Polynesia is in the Pacific Ocean at 16.758°S, 145.238°W (Figure 3).  
 283 The atoll has one lagoon, two reef flats, and 27 motu. Faaite has a total lagoon area of 233.37  
 284 km<sup>2</sup>, reef flat area of 52.27 km<sup>2</sup>, and land area (motu area) of 11.48 km<sup>2</sup>. The two reef flats are  
 285 unequal in size with the primary reef flat accounting for more than 99% of the total reef flat area  
 286 (Figure 3a). The large standard deviation on the effective reef flat width measurements for Faaite  
 287 occurs because the distribution of widths is not unimodal. Seven of the motu are large enough to  
 288 calculate length and width measurements (Figure 3c). Similar to many atolls in our database, the  
 289 lagoon-side motu length is longer than the ocean-side motu length (6/7, Figure 3c). This is

exemplified in M4, where the lagoon-side motu length is 75% longer than the ocean-side motu length, as the lagoon side shoreline is more crenulated than the ocean-side shoreline. We see that the larger motu (plotted in green, Figure 3) are distributed on the northern shoreline while the smaller motu (only simple morphometrics, plotted in yellow Figure 3) are found mostly on the southern shorelines. To quantify this observation, we also bin all morphometrics relative to relative cardinal position on the atoll (Figure S1, Figure 4).

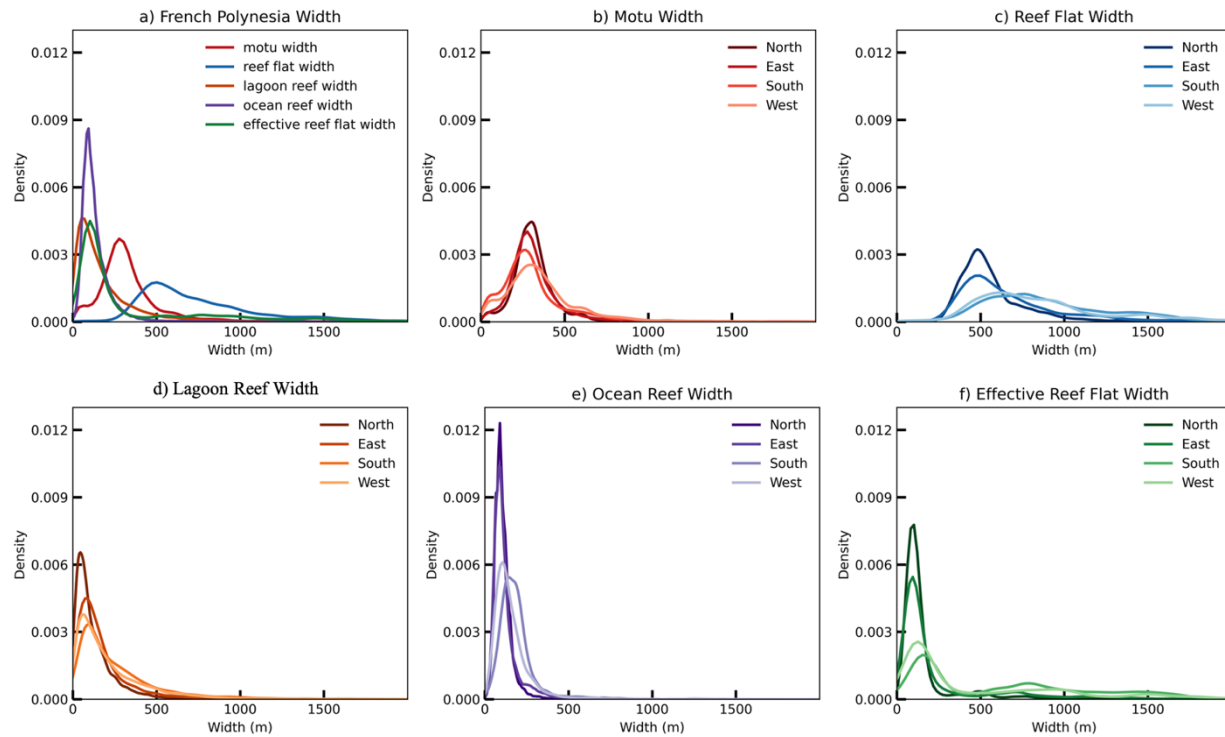


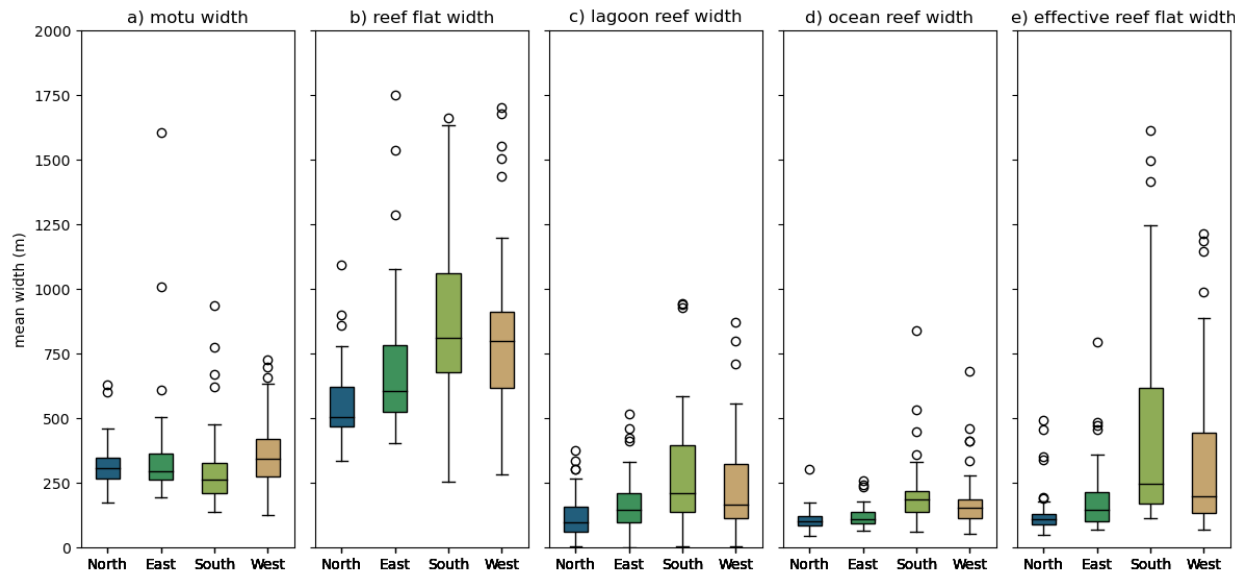
Figure 4. Density functions for width calculations in French Polynesia on a per-point basis. a) Atoll wide widths, binned by cardinal directions for b) motu width, c) total reef flat width, d) lagoon reef width, e) ocean reef width, and f) effective reef flat width.

### 3.2 Regional Scale Results: French Polynesia

There are 60 atolls in French Polynesia with sufficient Landsat coverage to create a temporal composite and calculate morphometrics. These atolls are located between  $14^{\circ} 24' S$ - $23^{\circ} 21' S$  and  $134^{\circ} 29' W$ - $154^{\circ} 41' W$ . These atolls have 1,930 motu (837 full morphometrics) and 80 reef flats (Table S1). In French Polynesia, there is on average 1.3 reef flat per atoll with the number of motu ranging from as few as 1 to as many as 69 and an average of 14 larger motu per atoll. 75% of the reef-flat length is blocked by motu length.

On a per-point basis, the ocean reef width has the narrowest distribution (Figure 4a&e) and the total reef width has the widest distribution (Figure 4a&c). When breaking out the data by cardinal position on the atoll, we see a clear trend that the northern shoreline consistently has the smallest range of widths while the south and west tend to have the widest range of measurements. When looking at motu width, ocean reef width, and lagoon reef width, there is a

312 strong unimodal distribution (Figure 4d&e). However, in the south and west direction, the reef  
 313 flat width measurements show a bimodal behavior (Figure 4c&f).



314  
 315 Figure 5. Cardinal position within the atoll binned widths in French Polynesia on a per-atoll basis for a) motu width,  
 316 b) reef flat width, c) lagoon reef width, d) ocean reef width, and e) effective reef flat width. One point per atoll is the  
 317 mean width. Not shown on total reef flat width (b), two outliers: one point at 2,790 m in the South bin and one at  
 318 2,320 m in the West bin.

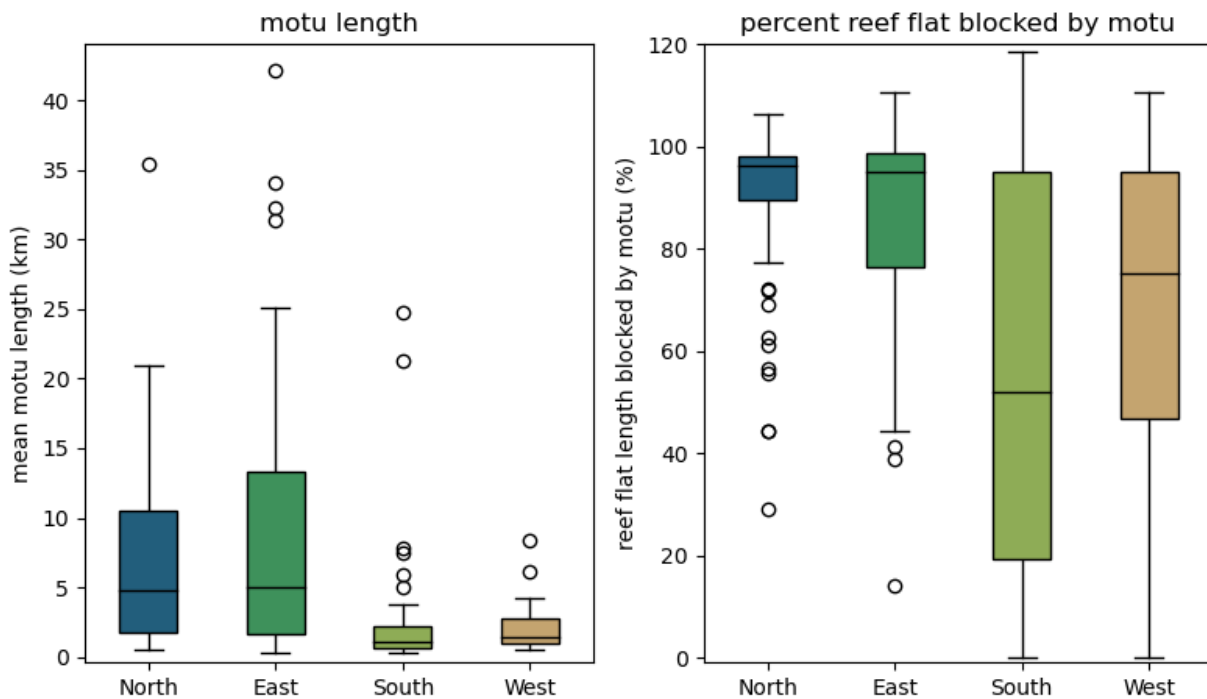
319 On a per-atoll basis (one data point per-bin per-atoll), small and large atolls are weighted  
 320 equally (Figure 5 and Figure 6). Median motu width range from 263 m in the south to 345 m in  
 321 the west (Figure 5a). The reef flat width is narrower in the north and east and wider in the south  
 322 and west with the largest variation in the south (Figure 5b). This trend is also observed in the  
 323 effective reef flat width, with the narrowest width in the north and the largest in the south (Figure  
 324 5e). The lagoon reef width (Figure 5c) is more variable than the ocean reef width (Figure 5d).  
 325 The north has the narrowest lagoon reef width of 100 m and the narrowest ocean reef width at  
 326 101 m. The south bin has the widest widths for both the mean lagoon reef width and the mean  
 327 ocean reef width at 212 m and 184 m respectively.

328  
 329 Table 1. Median with one standard deviation per atoll cardinal position binned for French Polynesia motu and reef-  
 330 flat morphometrics.

Cardinal Position	Ocean Reef Width (m)	Motu Width (m)	Lagoon Reef Width (m)	Reef Flat Width (m)	Effective Reef Flat Width (m)	Motu Length (km)	Length Blocked By Motu (%)
NORTH	101 ± 34	308 ± 77	100 ± 66	504 ± 85	109 ± 34	10.6 ± 1.33	96.2
EAST	108 ± 46	296 ± 98	145 ± 95	607 ± 175	147 ± 72	11.5 ± 1.80	95.1
SOUTH	185 ± 64	263 ± 103	212 ± 120	812 ± 123	248 ± 159	3.1 ± 0.47	51.8
WEST	154 ± 64	345 ± 148	166 ± 103	799 ± 168	200 ± 123	4.6 ± 1.22	75.3

331 The east and the north shores have the longest motu while the south and west have  
 332 shorter ones (Figure 6a). The north and the east have different morphometrics that reflects the  
 333 longer motu lengths including the tighter distribution of width measurements for the ocean reef  
 334 width reflecting less potential edge effects (Figure 4e). The north and east sides also have a  
 335 larger percent of their lengths covered by motu (Figure 6b). In the north and east a larger  
 336 percentage of the motu blocking access to the lagoon, and the overall reef flat width is narrower  
 337 (Table 1). Overall, in French Polynesia the north and east shores have longer motu and narrower

338 reef flats for all reef measurements (reef flat width, lagoon reef width, ocean reef width, and  
 339 effective reef flat width) compared to the south and west shores.



340  
 341 Figure 6. Binned directionally per-atoll mean motu length for French Polynesia Atolls. If a motu crosses in to more  
 342 than one bin it is included in the bin where it has the greatest number of ocean points. b) Percent length of reef flat  
 343 covered by motu separated by cardinal directional bin.

### 344 3.3 Global Scale Results

345 Morphometrics are calculated for 154 atolls (Figure 1). Overall, there are 3,795 motu  
 346 (1,753 with all morphometrics calculated) and 596 reef flats (Table 2). The total land (motu) area  
 347 is 1,836.55 km<sup>2</sup> and the total reef flat area is 7,387.43 km<sup>2</sup>.

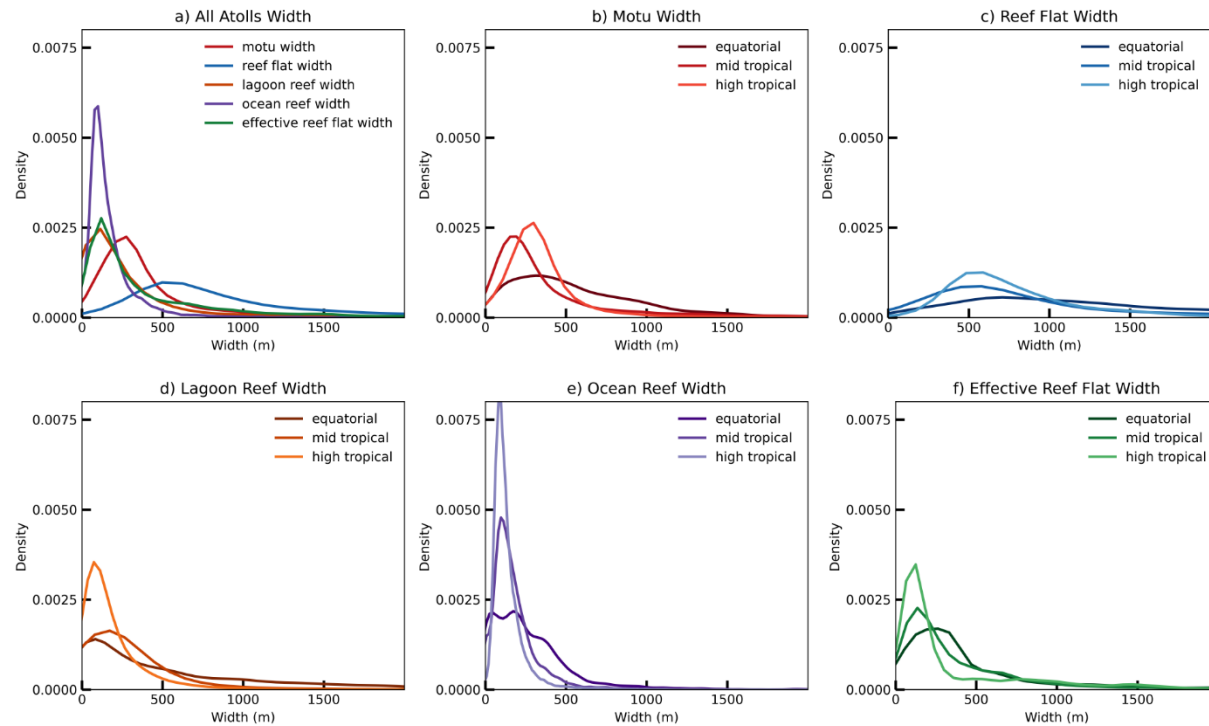
348

349 Table 2. Median morphometrics with one standard deviation per atoll binned by latitude for all atolls.

Bin	Atoll #	Motu #	Reef Flat #	Motu Area (km <sup>2</sup> )	Reef Flat Area (km <sup>2</sup> )	Motu Length (km)
LOW	31	184/395	118	3.8 ± 1.09	34.9 ± 0.31	3.9 ± 1.23
MID	57	695/1416	351	0.8 ± 0.49	20.1 ± 6.25	2.4 ± 1.06
HIGH	66	874/1994	127	2.9 ± 1.37	22.3 ± 0.60	8.8 ± 4.01
ALL	154	1753/3795	596	2.7 ± 0.98	27.4 ± 2.18	3.9 ± 2.10

350 Atolls are binned by their absolute latitudes, with the least number of atolls in the  
 351 equatorial latitudes (Table 2). The equatorial atolls are located from 4.7°S to 4.7°N, the mid  
 352 tropical atolls are from 14°S to 4.7°S and 4.7°N to 14°N, and the high tropical atolls are located  
 353 greater than 14°S and 14°N. The high tropical atolls are all located in the Pacific Ocean in the  
 354 southern hemisphere and are dominated by the atolls of French Polynesia (n=60/66). The  
 355 equatorial atolls have the least number of motu and reef flats per atoll with an average of 12.7  
 356 motu (5.9 motu with all morphometrics) and 3.4 reef flats. Mid tropical and high tropical atolls

357 have an average 24.4 motu (12.0 motu) and 6.1 reef flats, and 30.2 motu (13.1 motu) and 9.0 reef  
 358 flats respectively.



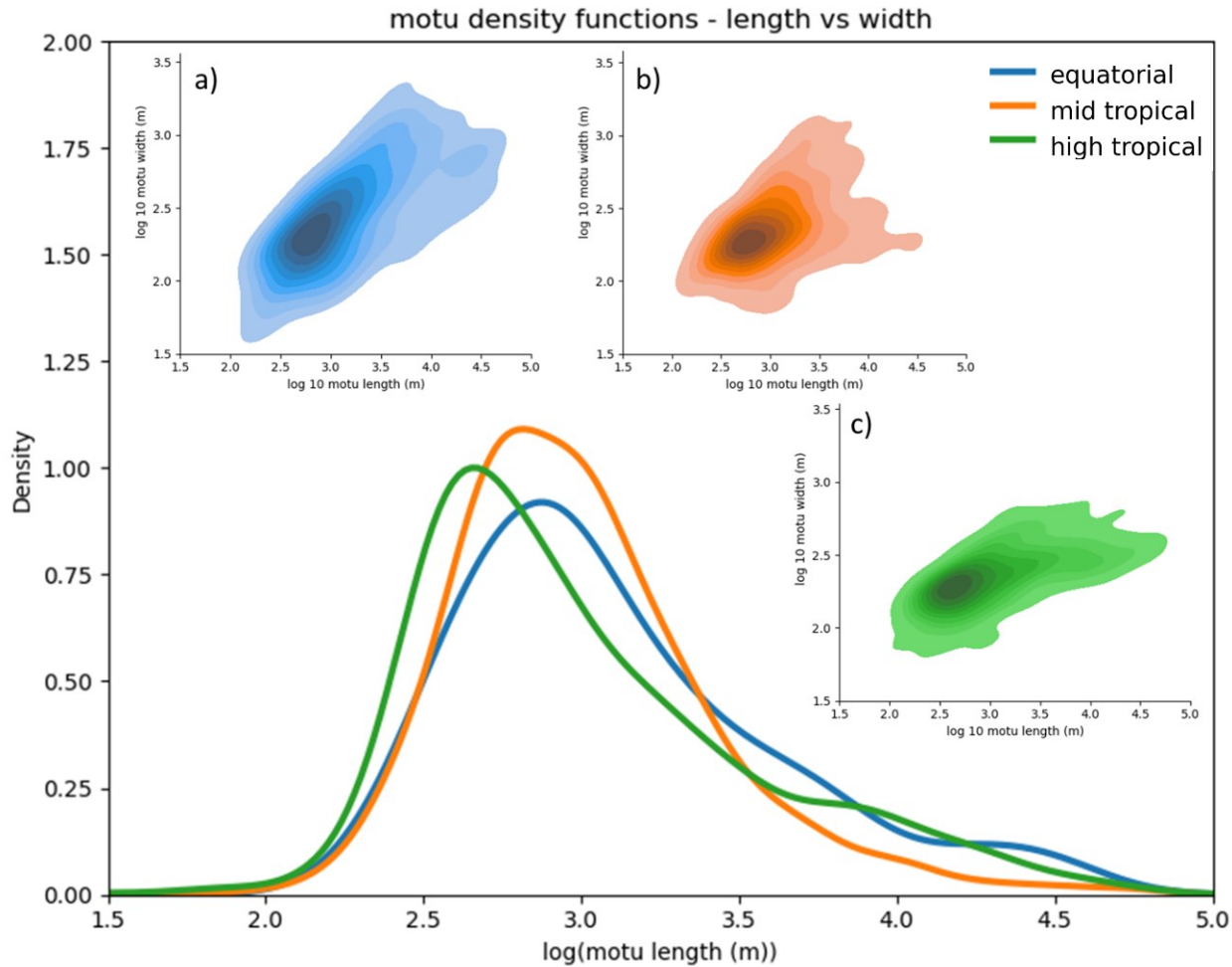
359

360 Figure 7. Density function of width measurements for all atolls on a per-point basis grouped by latitude. a) atoll  
 361 b) motu width, c) total reef flat width, d) lagoon reef flat width, e) ocean reef flat width , and f)  
 362 effective reef flat width.

363 The ocean reef width has the narrowest distribution of widths indicating that it varies the  
 364 least across all atolls (Figure 7a). The total reef flat width has the widest distribution. Equatorial  
 365 atolls consistently have lower peak densities, and thus have a wider distribution of widths  
 366 compared to our other two groups of atolls (Figure 7b-f). High tropical atolls have the narrowest  
 367 distributions of widths. The mid tropical atoll morphologies lie between the equatorial and high  
 368 tropical atolls with motu width and ocean reef width more closely aligned with the high tropical  
 369 atolls, while the effective reef flat width and lagoon reef width more closely match the equatorial  
 370 atolls. Ocean reef width for the equatorial atolls has a bimodal distribution with a skew toward  
 371 wider widths. Conversely, both mid and high tropical atolls show unimodal distributions (Figure  
 372 7e). The equatorial atolls also exhibit distinctly more skew towards wider motu (Figure 7b).

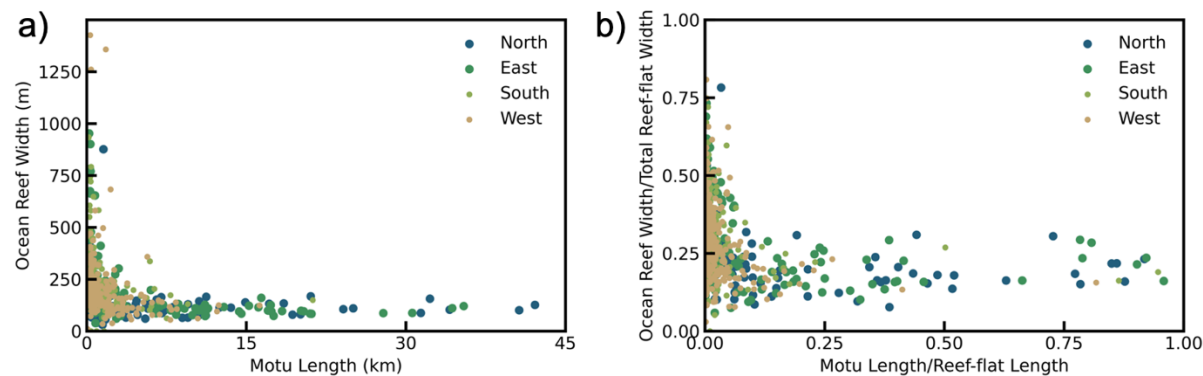
373 Mid tropical atolls have a narrower distribution of motu length than either equatorial or  
 374 high tropical atolls although their motu length peaks between them (Figure 8). High tropical  
 375 atolls have their peak length at a shorter motu length than the mid tropical or equatorial atolls.  
 376 When width is considered, the high tropical atolls have a narrower distribution of widths for the

377 longer motu (Figure 8c) as compared with larger distribution seen with the equatorial atolls  
 378 (Figure 8a).



379  
 380 Figure 8. Density function of motu length for all atolls on a per-motu basis grouped by latitude, with 2D distribution  
 381 of motu length and motu area for a) equatorial (blue), b) mid tropical (orange), and c) high tropical motu (green).

#### 382 4 Discussion



383  
 384 Figure 9. a) Reef flat width in front of motu (ocean reef width) vs motu length for each motu in French Polynesia  
 385 classified by cardinal position on the atoll. b) Reef flat width in front of the motu normalized by the width of the reef

flat the motu is on vs the motu length normalized by the length of the reef flat the motu is on classified by cardinal position on the atoll. Each point represents one motu.

On a per-object basis, the ocean reef width (reef width in front of the motu) reaches a near constant width once the motu reaches a certain length (Figure 9 and 10). For all French Polynesia motu longer than 1 km, the ocean reef width is  $150 \pm 110$  m ( $n = 324/837$ ), however the error drops into a quarter if we only look at motu longer than 10 km while the average reef-flat width in front of the motu remains similar ( $108 \pm 25$  m,  $n=54/837$ ) (Figure 9a). There are clear trends of increased numbers of large motu on the Northern and Eastern shores (52% and 45% respectively compared to only 29% and 36% on the Southern and Western sides), with starker differences for the longest motu  $> 10$  km (10-17% on N and E, with only 1-2% on S and W). The relative ocean reef width in front of the motu (Figure 9b) was calculated to ensure that smaller overall atoll footprints were not excluded. The same trend of a constant ocean reef width is exhibited again, dominated by Northern and Eastern motu (blue and green dots, Figure 9b). For motu that occupy more than 10% of the total reef-flat length, there is an average of 18% of the reef-flat width in front of the motu ( $n = 97/837$ ), with the majority (68/90) of these motu found on the N and E shores (70%). For smaller motu, i.e. with lengths  $< 1$  km, the mean ocean reef width is similar,  $202 \pm 138$  m, but with larger variation in ocean reef flat widths. The consistent pattern of near constant width in front of motu implies that self-organization may be driving a critical reef-flat width for French Polynesia.

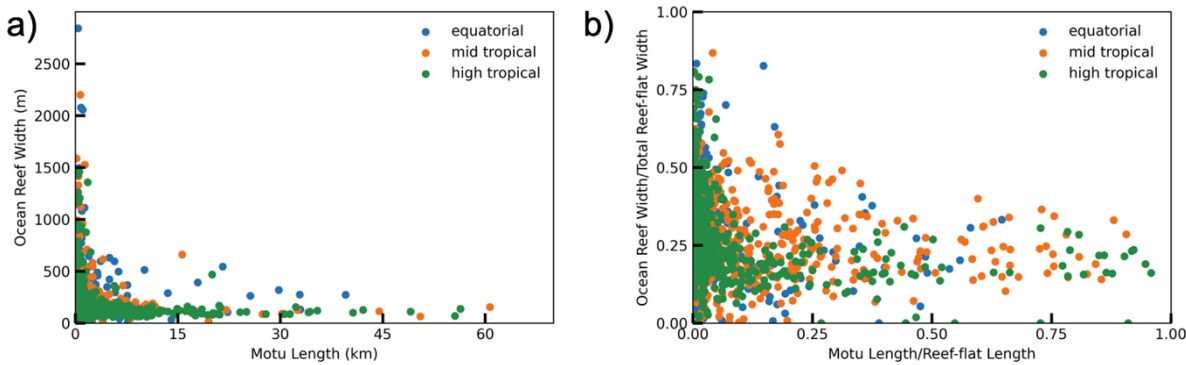
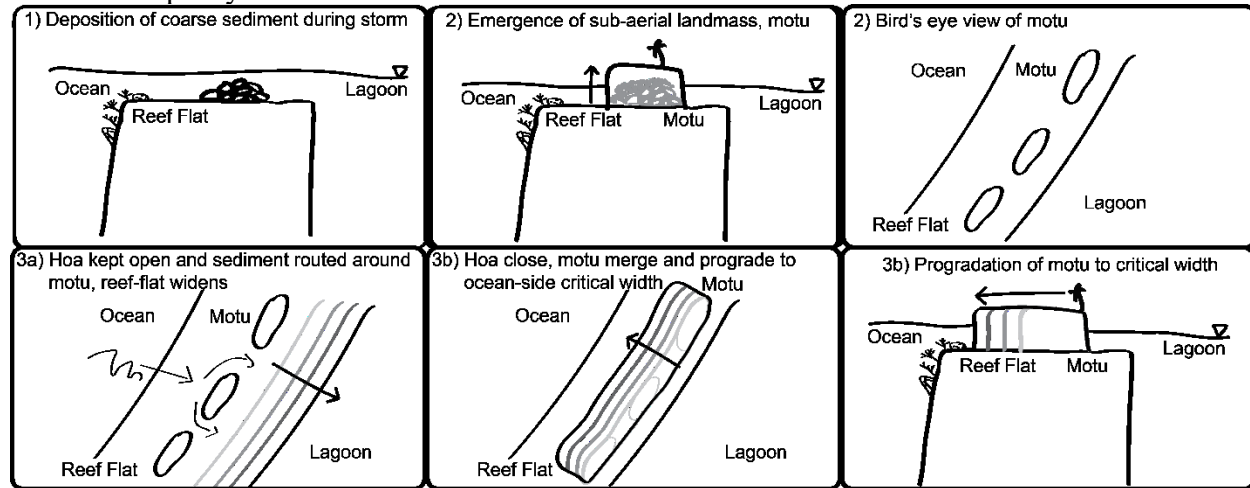


Figure 10. a) Reef flat width in front of motu (ocean reef width) vs motu length on a per motu basis classified by latitude. b) Reef flat width in front of the motu normalized by the width of the total reef flat under the motu vs the motu length normalized by the length of the reef flat the motu is on classified by latitude. Each point represents one motu classified as Equatorial Atolls (blue):  $0^\circ$  to  $4.7^\circ$ , Mid tropical atolls (orange):  $4.7^\circ$  to  $14^\circ$ , and High tropical atolls (green): greater than  $14^\circ$ .

This trend of a critical reef-flat width continues when looking at our global morphometrics of motu (Figure 10). For all motu  $> 1$  km in length, the mean ocean reef width is  $184 \pm 156$  m ( $n=725/1753$ ); and as the motu increase in length ( $> 10$  km), the error decreases to a mean ocean reef width of  $142 \pm 106$  m ( $n=89/1753$ ) (Figure 10a). There are variations between our different groups of atolls, with the equatorial atolls exhibiting a larger and more variable critical reef-falt width for all large motu ( $> 1$  km),  $282 \pm 273$  m, compared to the mid and high tropical atolls,  $193 \pm 140$  m and  $150 \pm 111$  m respectively (Figure 10a). However, when we normalize the motu by the size of the atoll (Figure 10b), we find that for motu occupying  $> 10\%$  of the total reef-flat length, the ocean reef width is about 22% of the total reef-flat width ( $n=331/1753$ ). Increasing the cutoff for only motu that occupy at least 25% of the reef flat length, the averages remain the same across all atoll groups (equatorial: 23%, mid tropical: 25%, and low tropical: 17%) but the errors decrease, as seen earlier with French Polynesia (Figure 9b). Our

423 results highlight that the equatorial atolls have wider reef-flats dominated by larger motu, but  
 424 still about a 5<sup>th</sup> of the reef-flat width remains open in front of all large motu across our 154 atolls.  
 425 This trend of a near constant reef-flat width in front of the motu implies that there maybe an  
 426 equilibrium ocean reef width in front of large motu as suggested by Ortiz and Ashton (2019)  
 427 modeling in Xbeach. A key assumption to their conceptual model is that the motu modeled were  
 428 long-enough to not be affected by flow around the motu into the lagoon; thus long motu are the  
 429 best natural proxy.



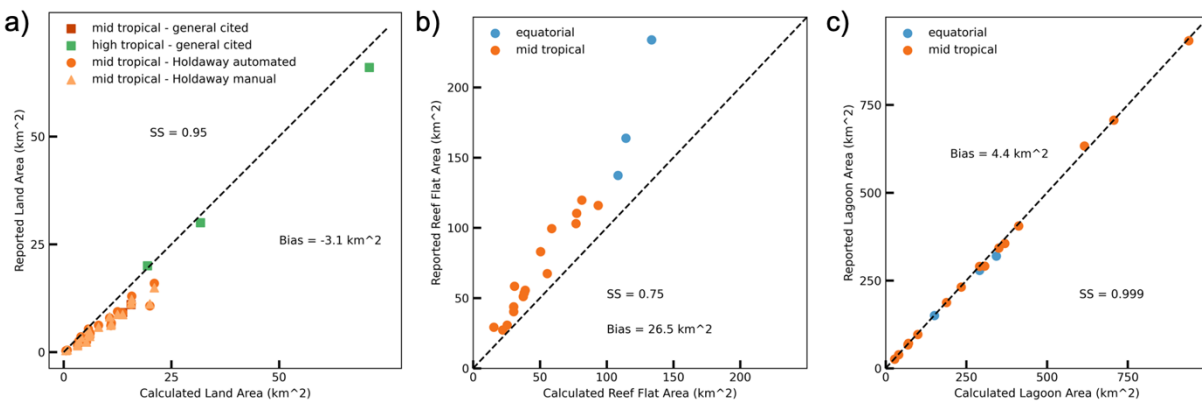
430  
 431 Figure 11. Conceptual model of motu formation and evolution on the reef flat adapted from Ortiz and Ashton (2019)  
 432 from initial motu creation and emergence (1-2) to divergence of motu evolution leading to widening of the  
 433 underlying reef-flat (3a) or narrowing of the motu to ocean side reef flat (ocean reef width) with elongated motu  
 434 (3b).

435 Using the data generated, we quantify motu and reef flats morphometrics as well as tease  
 436 out potential patterns in morphology and possible causes. Building upon Ortiz and Ashton's  
 437 (2019) conceptual model of motu formation and evolution, we propose an updated model to  
 438 account for varying patterns seen globally in our dataset (Figure 11). Motu formation starts with  
 439 the deposition of coarse sediment near the mid-point of the reef-flat evolving to a sub-aerial  
 440 landmass (Figure 11.1-2). Once there are several motu along a section of reef flat, the system  
 441 may evolve in two ways. If the motu stay separate, i.e. the shallow channels between the motu  
 442 (also called by the Polynesian term, hoa) stay active, the sediment supply from ocean-side reefs  
 443 will cause the reef flat to prograde towards the lagoon and widen over time (Figure 11.3a). If the  
 444 motu merge, such that sediment can no longer pass to the lagoon around the motu, that same  
 445 sediment supply should prograde the motu oceanwards as predicted by Ortiz and Ashton's  
 446 XBeach modeling (Figure 11.3b). The progradation and widening of the motu will continue until  
 447 the reef flat in front of that motu reaches a critical width (our measurement of ocean reef width).  
 448 The proposed conceptual model is one explanation for the lagoon vs ocean shoreline length  
 449 differences found that were discussed for Faaite. As motu merge both shorelines will be  
 450 sinusoidal, but as the ocean side prograde the shoreline will start to smooth and parallel the  
 451 shoreline of reef flat on the ocean-side, while the lagoon side will stay sinusoidal.

452 When a motu is long enough, the distance from the motu to the ocean-side reef flat  
 453 reaches a near constant width (Figure 9&11). When considered directionally, the northern and  
 454 eastern shores of the French Polynesia atolls consistently have more motu that are considerably  
 455 longer (10-11 km) and block a larger percentage of the reef flat (95-96%) than the south and  
 456 western sides (3-4.5 km and 52-75%, Table 1). Moreover, the total reef flat tends to be narrower

457 as does the ocean reef width (critical reef-flat width in front of the motu) on the N and E  
 458 compared to the S and W with less variability in the measurements (Figure 5 and Table 1). While  
 459 on the Southern and Western sides, the reef flat width has a bimodal distribution with a  
 460 secondary peak occurring at a wider width of ~1.5 km (Figure 4c). As the north and east have  
 461 around 95% of the reef flat length blocked by motu, with only 52% percent blocked in the south,  
 462 there is a clear correlation between length of motu blocked and reef flat width.

463 While our database covers an extensive range of atolls and morphometrics, it is limited to  
 464 almost half of the available temporal composites created. In addition, another 100-200 locations,  
 465 typically considered atolls (Bryan, 1953; Goldberg, 2016), are not currently measured here due  
 466 to lack of available quality composites. Only atolls with sufficient Landsat coverage had  
 467 temporal composites created, and some atolls with a more fractal-like morphology (i.e. parts of  
 468 the Maldives) were not able to be run in our morphometric code. This resulted in using atolls  
 469 primarily from the Pacific Ocean that have clearly defined lagoons. We are also biased towards  
 470 larger motu due to the 30m resolution of the Landsat imagery and the size of motu and reef flat  
 471 necessary to run the full morphometric code. Lastly, several assumptions are made in our current  
 472 code that limit its flexibility from assuming that the most numerous area in our composite is  
 473 water to assuming that there are only three dominant landcover classes and that k-means  
 474 unsupervised classification is the best method for classifying our image.



475  
 476 Figure 12. Validation of per-atoll morphometrics comparing calculated to previously reported morphometrics for a)  
 477 total land area, b) total reef-flat area, and c) total lagoon area with calculated Skill Score (SS) and Bias and 1:1 line  
 478 (black dashed).

479 In order to validate our methodology, we compared the calculated morphometrics  
 480 presented in this paper with values reported in previous studies on atolls (Figure 12). Similar to  
 481 Holdaway et al. (2021), we performed this validation at the atoll area scale using the bias (mean  
 482 error between previously reported morphometrics and our calculated morphometrics) and Brier  
 483 Skill Score (estimate of error in our morphometrics to variance of previously reported  
 484 morphometrics) (Gharagozlou et al., 2020). Our estimates of both reef-flat area and lagoon area  
 485 (Figure 12b&c) are consistently under-predicting the area with a bias of  $26.5 \text{ km}^2$  and  $4.4 \text{ km}^2$   
 486 respectively. However, our morphometrics over-predict total land area per atoll on average by

487 3.1 km<sup>2</sup> (Figure 12a). All our estimates of total area per atoll have an excellent Brier Skill Score  
 488 and follow reported previous landcover areas well.

## 489 **5 Conclusions**

490 We have developed a global database of atolls along with a methodology to  
 491 systematically create temporal Landsat composites and measure morphometrics of three  
 492 landcover classes (land, water, and reef flats). Our code enables quick and easy comparison  
 493 between different scales of our database from investigating the variability in motu  
 494 morphometrics at a single atoll to a regional grouping to a global analysis. With the use of  
 495 pandas dataframes, all the morphometrics can be grouped based on shoreline orientation, relative  
 496 position on the atoll, or per-object. We have highlighted several potential binning methods to  
 497 analyze the patterns found in our database (such as using the relative position on the atoll for  
 498 exploring the spatial heterogeneity of motu distributions in French Polynesia by segregating into  
 499 N, E, S, and W). Distinct and quantifiable differences were shown in the location of motu on  
 500 atolls within a region (French Polynesia) and globally based on latitude. The code to create  
 501 composites and measure morphometrics is available for other researchers to employ. This  
 502 automated analysis will allow for the direct comparison of data, providing one possible answer to  
 503 Duvat and Magnan's call for research priority of creating a common assessment protocol.  
 504 Further research includes extending the analysis of our dataset by comparing the morphometrics  
 505 with potential drivers such as waves, storms, and anthropogenic activities to explain differences  
 506 in the behavior for either directionality for a specific regions or different latitudes (i.e. in French  
 507 Polynesia wave climate and directionality of the motu widths, presence on the reef flat).

## 508 **Acknowledgments**

509 The authors acknowledge funding from the Southeast Climate Adaptation Science Center for F.  
 510 Johnson Global Change fellow. F. Johnson was primarily responsible for data curation, formal  
 511 analysis, software development, visualization, and writing the original draft. A. Ortiz was  
 512 primarily responsible for conceptualization of the project, funding acquisition, investigation,  
 513 methodology development, validation, project administration and supervision, and reviewing and  
 514 editing this paper. The authors would like to thank Sean Daly for the initial creation of the  
 515 inclusive Atoll Database.

## 516 **Open Research**

518 All software used in this project is open-source and freely available. Only freely available Landsat imagery  
 519 was used for each atoll composite. All python scripts referenced herein is available on the Github repository  
 520 [AtollGeoMorph](#). All the code needed to create the data visualization in Figures 5-10 and 12 is also available on  
 521 the AtollGeoMorph Github repository. All tables created can be extracted from the csv files generated by these  
 522 scripts.

## 523 **References**

525 Albert, S., Leon, J. X., Grinham, A. R., Church, J. A., Gibbes, B. R., & Woodroffe, C. D.  
 526 (2016a). Interactions between sea-level rise and wave exposure on reef island  
 527 dynamics in the Solomon Islands. *Environmental Research Letters*, 11(5), 054011.

- 528 Albert, S., Leon, J. X., Grinham, A. R., Church, J. A., Gibbes, B. R., & Woodroffe, C. D.  
 529 (2016b). Interactions between sea-level rise and wave exposure on reef island  
 530 dynamics in the Solomon Islands. *Environmental Research Letters*, 11(5), 054011.
- 531 Aslam, M., & Kench, P. S. (2017a). Reef island dynamics and mechanisms of change in  
 532 Huvadhoo Atoll, Republic of Maldives, Indian Ocean. *Anthropocene*, 18, 57–68.
- 533 Aslam, M., & Kench, P. S. (2017b). Reef island dynamics and mechanisms of change in  
 534 Huvadhoo Atoll, Republic of Maldives, Indian Ocean. *Anthropocene*, 18, 57–68.
- 535 Barnett, J., & Adger, W. N. (2003). Climate Dangers and Atoll Countries. *Climatic Change*,  
 536 61(3), 321–337. <https://doi.org/10.1023/B:CLIM.0000004559.08755.88>
- 537 Brander, R. W., Kench, P. S., & Hart, D. (2004). Spatial and temporal variations in wave  
 538 characteristics across a reef platform, Warraber Island, Torres Strait, Australia. *Marine  
 539 Geology*, 207(1–4), 169–184.  
<https://doi.org/http://dx.doi.org/10.1016/j.margeo.2004.03.014>
- 540 Bryan, E. H. Jr. (1953). A Check List of Atolls. *Atoll Research Bulletin*, (19), 1–38.
- 541 Daly, R. A. (1925). Pleistocene changes of level. *American Journal of Science*, (58), 281–  
 542 313. <https://doi.org/10.2475/ajs.s5-10.58.281>
- 543 Darwin, C. (1842). *On the Structure and Distribution of Coral Reefs: Being the First Part  
 544 of the Geology of the Voyage of the Beagle Under the Command of Captain Fitzroy,  
 545 RN During the Years 1832 to 1836*. Smith, Elder.
- 546 Duvat, V. K. E. (2019). A global assessment of atoll island planform changes over the past  
 547 decades. *Wiley Interdisciplinary Reviews: Climate Change*, 10(1), e557.
- 548 Duvat, V. K. E., & Magnan, A. K. (2019). Rapid human-driven undermining of atoll island  
 549 capacity to adjust to ocean climate-related pressures. *Scientific Reports*, 9(1).  
<https://doi.org/10.1038/s41598-019-51468-3>
- 550 Duvat, V. K. E., & Pillet, V. (2017). Shoreline changes in reef islands of the Central Pacific:  
 551 Takapoto Atoll, Northern Tuamotu, French Polynesia. *Geomorphology*.  
<https://doi.org/https://doi.org/10.1016/j.geomorph.2017.01.002>
- 552 Eyre, B. D., Cyronak, T., Drupp, P., de Carlo, E. H., Sachs, J. P., & Andersson, A. J.  
 553 (2018). Coral reefs will transition to net dissolving before end of century. *Science*,  
 554 359(6378), 908–911.
- 555 Fletcher, B. C. H., & Richmond, B. M. (2010). *Climate Change in the Federated States of  
 556 Micronesia: Food and Water Security, Climate Risk Management, and Adaptive  
 557 Strategies*. Retrieved from  
[http://seagrant.soest.hawaii.edu/sites/default/files/publications/1webfinal\\_maindocument\\_climatechangefsm.pdf](http://seagrant.soest.hawaii.edu/sites/default/files/publications/1webfinal_maindocument_climatechangefsm.pdf)
- 558 Ford, M. (2011). Shoreline Changes on an Urban Atoll in the Central Pacific Ocean: Majuro  
 559 Atoll, Marshall Islands. *Journal of Coastal Research*, 11–22.  
<https://doi.org/10.2112/JCOASTRES-D-11-00008.1>
- 560 Ford, M. R., & Kench, P. S. (2014). Formation and adjustment of typhoon-impacted reef  
 561 islands interpreted from remote imagery: Nadikdik Atoll, Marshall Islands.  
*Geomorphology*, 214, 216–222. <https://doi.org/10.1016/j.geomorph.2014.02.006>
- 562 Ford, M. R., & Kench, P. S. (2015). Multi-decadal shoreline changes in response to sea  
 563 level rise in the Marshall Islands. *Anthropocene*, 11, 14–24.  
<https://doi.org/https://doi.org/10.1016/j.ancene.2015.11.002>
- 564 Garcin, M., Vendé-Leclerc, M., Maurizot, P., le Cozannet, G., Robineau, B., & Nicolae-  
 565 Lerma, A. (2016). Lagoon islets as indicators of recent environmental changes in the

- 574 South Pacific—The New Caledonian example. *Continental Shelf Research*, 122, 120–  
575 140.

576 Gharagozlu, A., Dietrich, J. C., Karancı, A., Luettich, R. A., & Overton, M. F. (2020). Storm-  
577 driven erosion and inundation of barrier islands from dune-to region-scales. *Coastal  
578 Engineering*, 158, 103674. <https://doi.org/10.1016/J.COASTALENG.2020.103674>

579 Goldberg, W. M. (2016). ATOLLS OF THE WORLD: REVISITING THE ORIGINAL  
580 CHECKLIST. *Atoll Research Bulletin*, 2, (610).

581 Hoeke, R. K., McInnes, K. L., Kruger, J. C., McNaught, R. J., Hunter, J. R., & Smithers, S.  
582 G. (2013). Widespread inundation of Pacific islands triggered by distant-source wind-  
583 waves. *Global and Planetary Change*, 108, 128–138.

584 Holdaway, A., Ford, M., & Owen, S. (2021). Global-scale changes in the area of atoll  
585 islands during the 21st century. *Anthropocene*, 33, 100282.

586 Kench, Paul S, McLean, R. F., & Nichol, S. L. (2005). New model for reef-island evolution:  
587 Maldives, Indian Ocean. *Geology*, 33.

588 Kench, Paul S, Ford, M. R., & Owen, S. D. (2018). Patterns of island change and  
589 persistence offer alternate adaptation pathways for atoll nations. *Nature  
590 Communications*, 9(1), 605. <https://doi.org/https://doi.org/10.1038/s41467-018-02954-1>

591 Kench, Paul Simon, Owen, S. D., & Ford, M. R. (2014). Evidence for coral island  
592 formation during rising sea level in the central Pacific Ocean. *Geophysical Research  
593 Letters*, 41(3), 820–827. <https://doi.org/10.1002/2013GL059000>

594 Kench, Paul Simon, Chan, J., Owen, S. D., & McLean, R. F. (2014). The geomorphology,  
595 development and temporal dynamics of Tepuka Island, Funafuti atoll, Tuvalu.  
596 *Geomorphology*, 222, 46–58. <https://doi.org/10.1016/j.geomorph.2014.03.043>

597 Kench, Paul Simon, Beetham, E., Bosserelle, C., Kruger, J., Pohler, S. M. L. M. L., Coco,  
598 G., & Ryan, E. J. J. (2017). Nearshore hydrodynamics, beachface cobble transport and  
599 morphodynamics on a Pacific atoll motu. *Marine Geology*, 389, 17–31. Retrieved from  
600 <https://www.sciencedirect.com/science/article/pii/S0025322716303668>

601 Kumar, L. (Ed.). (2020). *Climate Change and Impacts in the Pacific*. Cham: Springer  
602 International Publishing. <https://doi.org/10.1007/978-3-030-32878-8>

603 Mateo-García, G., Gómez-Chova, L., Amorós-López, J., Muñoz-Marí, J., & Camps-Valls,  
604 G. (2018). Multitemporal Cloud Masking in the Google Earth Engine. *Remote Sensing*,  
605 10(7), 1079. <https://doi.org/10.3390/rs10071079>

606 McLean, R., & Kench, P. (2015a). Destruction or persistence of coral atoll islands in the  
607 face of 20th and 21st century sea-level rise? *Wiley Interdisciplinary Reviews: Climate  
608 Change*, 6(5), 445–463. <https://doi.org/10.1002/wcc.350>

609 McLean, R., & Kench, P. (2015b). Destruction or persistence of coral atoll islands in the  
610 face of 20th and 21st century sea-level rise? *Wiley Interdisciplinary Reviews: Climate  
611 Change*, 6(5), 445–463.

612 Nunn, P. D., Kumar, L., McLean, R., & Eliot, I. (2020). Islands in the pacific: Settings,  
613 distribution and classification. In *Springer Climate* (pp. 33–170). Springer.  
614 [https://doi.org/10.1007/978-3-030-32878-8\\_2](https://doi.org/10.1007/978-3-030-32878-8_2)

615 Ortiz, A. C., & Ashton, A. D. (2019). Exploring carbonate reef flat hydrodynamics and  
616 potential formation and growth mechanisms for motu. *Marine Geology*, 412, 173–186.  
617 <https://doi.org/10.17605/OSF.IO/R3J2D>

618

- 619 Ortiz, A. C., Roy, S., & Edmonds, D. A. (2016). Marsh collapse by pond expansion on the  
 620 Mississippi River Delta Plain. *Nature Geosciences*, submitted.
- 621 Ortiz, A. C., Roy, S., & Edmonds, D. A. (2017). Land loss by pond expansion on the  
 622 Mississippi River Delta Plain. *Geophysical Research Letters*, 44(8), 3635–3642.  
 623 <https://doi.org/10.1002/2017GL073079>
- 624 Perry, C. T., Kench, P. S., Smithers, S. G., Yamano, H., O'Leary, M., & Gulliver, P. (2013).  
 625 Time scales and modes of reef lagoon infilling in the Maldives and controls on the  
 626 onset of reef island formation. *Geology*, 41(10), 1111–1114.  
 627 <https://doi.org/10.1130/G34690.1>
- 628 Richmond, B. M. (1992). Development of atoll islets in the central Pacific. In *Proceedings*  
 629 *of the 7th international coral reef congress* (Vol. 2, pp. 1185–1194).
- 630 Schlager, W., & Purkis, S. J. (2013). Bucket structure in carbonate accumulations of the  
 631 Maldives, Chagos and Laccadive archipelagos. *International Journal of Earth Sciences*,  
 632 102(8), 2225–2238. <https://doi.org/10.1007/s00531-013-0913-5>
- 633 Sengupta, M., Ford, M. R., & Kench, P. S. (2021). Shoreline changes in coral reef islands of  
 634 the Federated States of Micronesia since the mid-20th century. *Geomorphology*, 377,  
 635 107584.
- 636 Shope, J. B., & Storlazzi, C. D. (2019). Assessing morphologic controls on atoll island  
 637 alongshore sediment transport gradients due to future sea-level rise. *Frontiers in*  
 638 *Marine Science*, 6, 245.
- 639 Shope, J. B., Storlazzi, C. D., & Hoeke, R. K. (2017). Projected atoll shoreline and run-up  
 640 changes in response to sea-level rise and varying large wave conditions at Wake and  
 641 Midway Atolls, Northwestern Hawaiian Islands. *Geomorphology*, 295, 537–550.  
 642 <https://doi.org/https://doi.org/10.1016/j.geomorph.2017.08.002>
- 643 Stoddart, D. R. (1965). The shape of atolls. *Marine Geology*, 3.
- 644 Storlazzi, C. D., Elias, E. P. L., & Berkowitz, P. (2015). Many atolls may be uninhabitable  
 645 within decades due to climate change. *Scientific Reports*, 5, 14546.
- 646 Toomey, M., Ashton, A. D., & Perron, J. T. (2013). Profiles of ocean island coral reefs  
 647 controlled by sea-level history and carbonate accumulation rates. *Geology*, 41(7), 731–  
 648 734. <https://doi.org/https://doi.org/10.1130/G34109.1>
- 649 Toomey, M. R., Ashton, A. D., Raymo, M. E., & Perron, J. T. (2016). Late Cenozoic sea  
 650 level and the rise of modern rimmed atolls. *Palaeogeography, Palaeoclimatology,*  
 651 *Palaeoecology*, 451, 73–83.
- 652 Webb, A. P., & Kench, P. S. (2010). The dynamic response of reef islands to sea-level rise:  
 653 Evidence from multi-decadal analysis of island change in the Central Pacific. *Global*  
 654 *and Planetary Change*, 72. <https://doi.org/10.1016/j.gloplacha.2010.05.003>
- 655 Woodroffe, C D, McLean, R. F., Smithers, S. G., & Lawson, E. M. (1999). Atoll reef-island  
 656 formation and response to sea-level change: West Island, Cocos (Keeling) Islands.  
 657 *Marine Geology*, 160(1–2), 85–104.
- 658 Woodroffe, Colin D., Samosorn, B., Hua, Q., & Hart, D. E. (2007). Incremental accretion of  
 659 a sandy reef island over the past 3000 years indicated by component-specific  
 660 radiocarbon dating. *Geophysical Research Letters*, 34(3), L03602.  
 661 <https://doi.org/10.1029/2006GL028875>